JOURNAL OF OPTOELECTRONICS AND ADVANCED MATERIALS Vol. 12, No. 3, March 2010, p. 500 - 504

# Laser nanostructuring of thin Au films for application in surface enhanced Raman spectroscopy

S. IMAMOVA[a], A. DIKOVSKA[a], N. NEDYALKOV[a,c], P. ATANASOV[a],
M. SAWCZAK[b], R. JENDRZEJEWSKI[b], G. ŚLIWIŃSKI[b], M. OBARA[c]
[a]*Institute of Electronics, Bulgarian Academy of Sciences, Tzarigradsko shousse 72, Sofia 1784, Bulgaria*
[b]*Photophysics & Laser Lab., IF-FM, Polish Academy of Science, 14 Fiszera St., 80-231 Gdansk, Poland*
[c]*Department of Electronics and Electrical Engineering, Faculty of Science and Technology, Keio University, 3-14-1 Hiyoshi, Kohoku-ku, Yokohama 223-8522, Japan*

This paper presents experimental results of excimer laser nanomodification of thin gold films. Films with different thicknesses and deposition conditions are produced on $SiO_2$ substrate by pulsed laser deposition technique. Laser annealing of the deposited thin films results in its nanostructuring as the film is decomposed into nanoparticles with diameters in the range of few tens of nanometers. The produced nanostructured surfaces are covered with Rodamine 6G and tested as active substrates for Surface Enhanced Raman Spectroscopy (SERS). The SERS enhancement factor is estimated as high as $10^7$. The explanation of the results is made on the basis of the properties of the electromagnetic field in the near field zone of the nanostructured surface described by Finite Difference Time Domain (FDTD) simulation technique.

(Received June 18, 2009; accepted November 19, 2009)

*Keywords:* Laser nanostructuring, Near field, SERS

## 1. Introduction

The properties of the electromagnetic field in the near field zone around the nanosized metal structures irradiated by laser pulse attract much attention recent years. The interest is based on the specific properties related to localization and enhancement of the field in close vicinity of the structure, as the spatial characteristic of this field are defined by the size of the structure, not by the incident wavelength [1]. The unique properties of the near field are used for construction of different systems for imaging, diagnostics, therapy and catalysis applications. Examples of such systems are scanning near field optical microscope [2] or tip enhanced Raman spectroscopy device [3] that have a resolution in nanometer scale.

One of the most important applications of the nanostructured metal surfaces is Surface-enhanced Raman spectroscopy (SERS), a technique for identification and structural characterization of substances [4,5]. The practical application of SERS is based on the signal enhancement which is several orders of magnitude higher compared to the normal Raman scattering (NR). Thus it allows measurements with very low analyte concentration and low laser intensity [6-8] which is one of the major limitation of NR scattering.

Among the different methods developed for fabrication of nanostructured surfaces are electron and ion beam lithography [9-11], direct laser 2D and 3D structuring [12-14], the use of enhanced near field around metal tip [15]. Femtosecond laser nanostructuring of silicon-based SERS substrates is also recently reported [16].

The nanostructuring of thin metal films by excimer laser pulses is introduced as a novel technique for the production of nanoparticles on $SiO_2$/Si and ITO/glass substrates by Henley et. al. [17, 18]. The fragmentation of the metal surface into nanosized droplets during the melting is due to of the poorly wetting between substrate and liquid phase. The priority of this technique is easily obtaining of structures with controllable dimensions of nanoparticles by standard apparatuses in the micro-electronic. These surfaces are characterized and with high purity. However, the efficient practical applications of the method and produced structures need more detailed investigation.

In this paper we investigate nanomodification of thin gold films on $SiO_2$ at different conditions of film deposition. We define experimental conditions that ensure thin film modifications with uniform spatial characteristics in a wide area. It is shown that the produced substrates can be used as active substrates for SERS analysis. The enhancement of the Raman signal is explained by the electric field distribution and the optical near-field enhancement in the vicinity of produced nanostructures.

## 2. Simulation

The description of the properties of the electromagnetic field in the near field zone of the produced structures is made by Finite Difference Time Domain Simulation [19]. This technique is a numerical algorithm for solving of Maxwell's equation and it allows the solution of electromagnetic distributions for complex

geometries and inhomogeneous systems. The simulated system is divided to elementary cells, where the electric and magnetic field components are calculated at each time step. The dielectric function of the gold particles is described by Drude model as the input parameters are taken from [20, 21]. Simulations are made for system that consists of gold nanoparticles placed on glass substrate. The structure of the nanoparticle array is taken from SEM image of the fabricated surfaces. The incident irradiation is a plane wave at wavelength of 785 nm, which corresponds to a standard Raman spectroscopy system. The dielectric function of the substrate is taken from Palik [22]. The electric field intensity which is an input parameter for FDTD simulation is assumed to be 1 $(V/m)^2$ in all simulations.

## 3. Experimental details

All gold films are produced by pulsed laser deposition on $SiO_2$ with excimer laser $\lambda$ = 308 nm, $\tau$ = 30 ns. The films are deposited at laser fluence of $F$ = 1.5 $J \cdot cm^{-2}$, ambient pressure of $4.10^{-3}$ Pa and at two temperatures of the substrate – room temperature $T_0$ and $T$ = 250 $^oC$. The deposition rate of 15 nm/min is estimated at the presented conditions. The film thicknesses are obtained by variation of the deposition time. Using the same excimer laser the films are annealed at the same environmental conditions. The laser annealing is performed at laser fluencies varied in the range of 100 to 280 $mJ \cdot cm^{-2}$ and number of pulses $N_p$= 20. The surfaces morphology of the samples is examined by field-emission scanning electron microscope (SEM). Micro-Raman system operated at 785 nm excitation is used to characterize the SERS properties of fabricated nanostructures. SERS measurements are carried out for Rodamine 6G dissolved in ethanol.

## 4. Results and discussion

The deposition conditions mentioned above ensure fabrication of thin gold films with minimal surface roughness and absence of defects. These parameters are found to be crucial for formation of structures with homogeneous size distribution of the formed nanoparticles. After UV laser deposition of the gold films they are annealed. The laser annealing leads to a fragmentation of the gold film and clear formation of nanoparticles. The fragmentation into droplets occurs if the liquid phase wets the substrate poorly. This is the case of gold on $SiO_2$ substrate [17]. The laser absorption leads to heating of the gold film. At certain fluence the film melts and due to the low interaction with the substrate it breaks up into nanosized droplets. The surfaces modification is performed at different laser fluencies in the range (100 ÷ 280) $mJ/cm^2$ for two initial thicknesses of the films $d \sim 60$ nm and 200 nm. Sequence of SEM images on Fig.1 shows this surfaces nanomodification. The nanostructured surfaces consist of nanosized spherical particles as the particle diameter depends on the incident laser fluence, deposition conditions, film thicknesses. These parameters can be used for an efficient control of the particle's density and its size distribution. The larger droplets are produced at lower fluence (Fig.1 (b)). The fluence in this case is found to be the threshold one for film modification. Fragmentation into much smaller droplets with high density are obtained at the higher fluencies (over threshold fluence) as shown Fig.1 **(c)**.

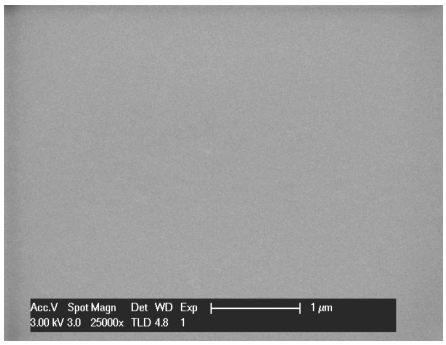


a

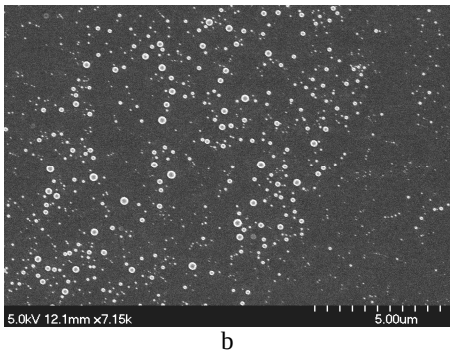


b

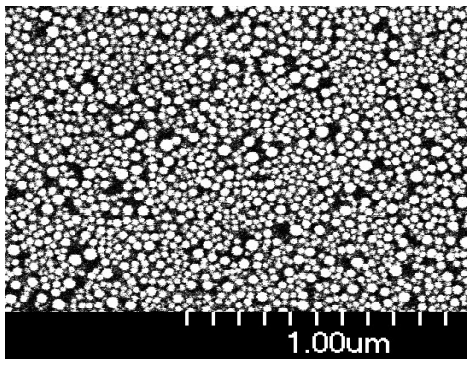


c

*Fig. 1 SEM images of annealed Au films with thickness $d \sim 60$ nm and deposited at $T_0$ (a) unannealed film, (b) F=100 $mJ.cm^{-2}$, Np=20, (c) F=130 $mJ.cm^{-2}$, Np = 20,*

The characteristics of the manufactured structures are found to depend on the conditions of film deposition. We can see the difference in the structures (a) and (b) on Fig. 2, which are deposited at different temperatures but annealed at the same conditions. The nanoparticles deposited at $T_0$ (Fig.2 (a)) are spherical with sizes in the

range 10nm ÷ 40nm, while these deposited at $T$ = 250 $^0$C are non - spherical and have sizes in the range of 20 ÷ 60 nm (Fig. 2 (b)). The difference in the observed structures may be related to the different degree of crystallinity that is influenced by the substrate temperature. Furthermore the seeds of thin film transformations in to nanoparticles are the domains that compose the film. The properties of these domains are also affected by the substrate temperature.

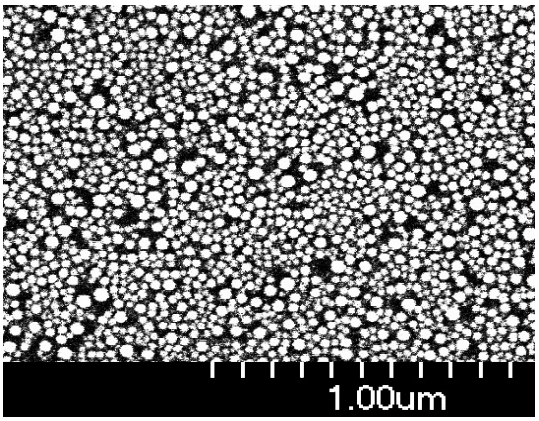


**a**

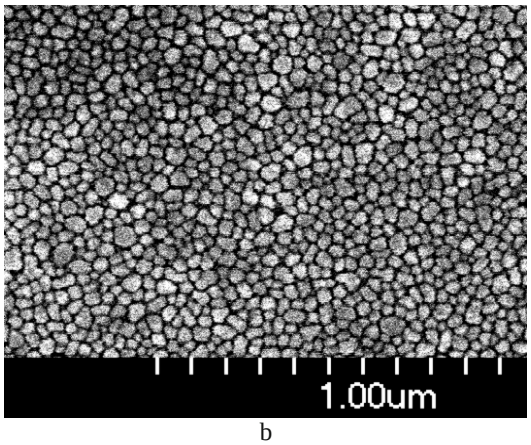


b

*Fig. 2 Annealed Au films with thickness d ~ 60 nm at F = 130 mJ.cm$^{-2}$ and Np = 20 of (a) deposited film at $T_0$ and (b) deposited at T =250 $^0$C.*

The film thicknesses also influence on size of the obtained nanoparticles. The nanoparticles sizes on Fig. 3 (a) and (b**)** produced at the same laser fluence for two different thicknesses 60 nm and 200 nm are about (30 ÷ 40) nm and (200 ÷ 400) respectively**.** It should be mentioned that recent results [23] show size-dependence of SERS enhancement from well-ordered and close-packed 2D nanostructure of gold nanoparticles. The dependence shows that SERS intensity is highest for nanoparticles with diameter in the range of (30 ÷ 100) nm as the maximal enhancement is for size of about 60 nm.

***(45$^0$)*View**

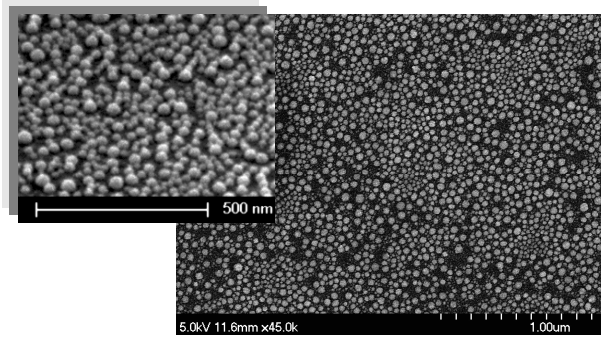


a

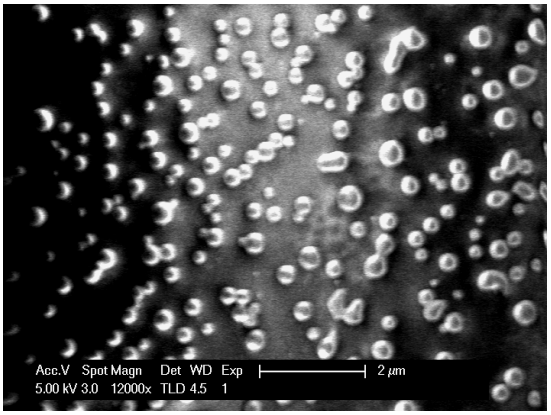


b

*Fig. 3 SEM images of annealed gold films (deposited at room temperature $T_0$ ) at F = 280 mJ.cm$^{-2}$, Np = 20 with thicknesses: (a) d = 60 nm , (b) d = 200 nm*

The optical properties in UV and visible spectral range of the noble metal nanoparticles are defined by the excitation of plasmon. The resonance wavelength of the plasmon excitations can be controlled by varying the shape and sizes of the nanostructures. This characteristic is especially important for SERS applications, since the efficient plasmon excitation is crucial for enhancement of the Raman signal. The absorption spectra of two of fabricated structures deposited at different substrate temperatures (room and 250$^0$C) are shown in Fig. 4 (a) and (b) respectively. The position of the maximum absorption for both samples is about 560nm. The higher absorption in (b) can be explained by the higher particle density observed in Fig. 4 (b).

The formation of nanostructured thin films with a homogeneous distribution of nanoparticles suggests that these structures can be used as effective SERS substrates with predictable optical properties. The produced structures in this study are tested as SERS substrates and Rodamine 6G as the active element is used.

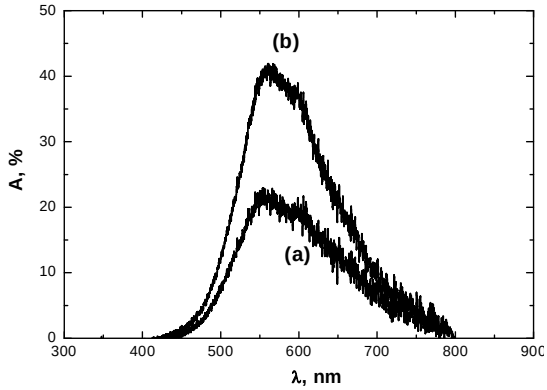


*Fig. 4. Absorption spectra of the nanostructured substrates (a) and (b) from Fig.2 .*

Fig. 5 shows Raman spectra of R6G deposited on glass (NR) and nanostructured substrates deposited at different conditions. The direct comparison between spectra of the NR and SERS spectra (a) and (b) on Fig. 5 shows the magnitude of the enhanced signal. For example the ratio of the intensities $I_{SERS}$ to $I_{NR}$ for spectra (b) shows essential enhancement of the Raman signal by a factor of about *~ 25.0 , 21.0 , 17.0* and *11.0* for *610 cm*$^{-1}$, *773 cm*$^{-1}$, *1180 cm*$^{-1}$, *1363 cm*$^{-1}$ respectively. As can be seen on Fig. 5 no fluorescent signal at excitation wavelength 785 nm is observed.

Metal nanostructures having junctions can produce large EM enhancement and they are better for SERS applications [24]. This is confirmed by comparison of the signals (a) and (b) on Fig. 5. The explanation for higher SERS enhancement of (b) is higher particle density and existence of junctions of the nanostructure (Fig.2 (b)) compared to the case of thin film deposited at room temperature (Fig. 2 (a)).

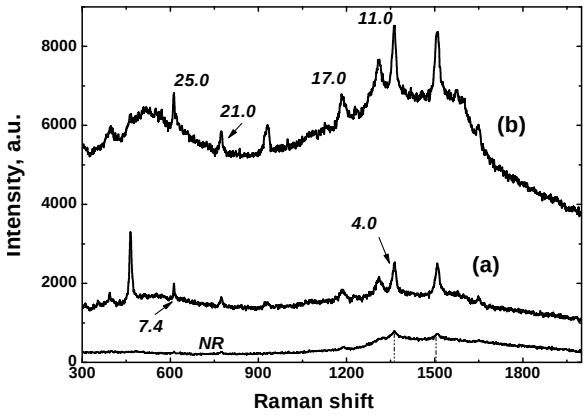


*Fig. 5 A comparison of the NR and SERS spectra of R6G adsorbed on substrates (a) and (b) shown on Fig. 2.*

In order to clarify the mechanism of signal enhancement for nanostructured surface an analysis of the electromagnetic field distribution in the near field zone is made on the basis of FTDT simulation. The theory of SERS predicts a power law between the signal intensity and the intensity of the incident irradiation. The simulated nanostructured area by FDTD is shown on Fig. 6. The area containing 19 spherical nanoparticles with sizes 30 nm ÷ 40 nm that are arranged on $SiO_2$ substrate with distances between them 5 nm ÷ 20 nm. The structure of the simulated system is taken from SEM image of the experimentally produced modified thin film (shown in the insert). The FDTD simulation of the near field distribution in the vicinity of the nanostructured surfaces show presence of "hot spots" where the intensity is enhanced by more than order of magnitude compared to the incident one. Near field intensity is higher for closely separated nanoparticles as it is seen on Fig. 6. Thus, the intensity enhancement realized in the "hot spots" efficiently excites the R6G molecules and that give and increase of the Raman signal for structured surface.

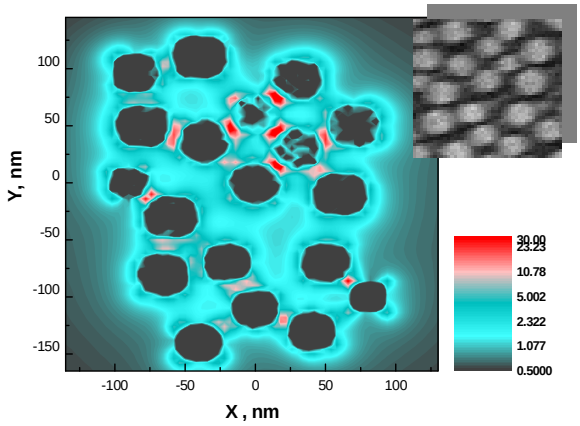


*Fig. 6 Calculated near field intensity distribution in the vicinity of Au nanoparticle array. The insert shows SEM image of the experimentally produced structure that is used for construction of the simulated system. The area containing 19 spherical nanoparticles with sizes 30 nm ÷ 40 nm which are arranged on $SiO_2$ substrate with distances between them 5 nm ÷ 20 nm. The color scale shows the ratio between the obtained and the incident field intensity*

## 5. Conclusions

The excimer laser annealing with $\lambda = 308$ *nm* and $\tau$ = 30 ns of thin gold films leads to formation of nanoparticles with narrow size distribution. The parameters of the produced structures can be modified by laser fluence, film thicknesses and by the conditions of film deposition.

The fabricated nanostructured Au surfaces are successfully utilized as substrates for SERS measurements. The enhancement factor is estimated in the range of $10^6 \div 5.10^7$. The distribution of the EM field estimated by FDTD indicates that the enhancement of

Raman signal can be explained by the near field intensity enhancement.

**Acknowledgments**

The authors acknowledge the financial support of Bulgarian Ministry of Education and Science under contract DO 02-293/08, International agreement between Bulgarian and Polish Academy of Sciences and Grant-in-Aid for the 21st Century COE for Optical and Electronic Device Technology for Access Network from MEXT in Japan.

## References

[1] S. Kawata (Ed.), Springer, Berlin, 2001.
[2] S. Patane, A. Arena, M. Allegrini, L. Amdereozzi, M. Faetti, M. Giordano, Opt. Comm. **210**, 37 (2002).
[3] J. Wessel, J. Opt. Soc. Am. **B 2**, 1538 (1985).
[4] K. Kneipp, H. Kneipp, I. Itzkan, R. R. Fasari, M. S. Feld, J. Phys., Condense. Matter **14**, R597 (2004).
[5] M. De Jesus, K. S. Giesfeldt, M. Sepaniak, J. Raman Spectrosc. **35**, 895 (2004).
[6] K. Kneipp, Y. Wang , H. Kneipp , L. T. Perelman, I. Itzkan, R. Dasari , Phys Rev. Lett **78**, 1667 (1997).
[7] K. Kneipp, H. Kneipp, R. Manoharan, I. Itzkan, R. Dasari et. al. , J Raman Spectrosc. **29**, 743, (1998).
[8] J. Jiang, Bosnick K., maillard M., Brus L., J. Phys. Chem. B **107,** 9964 (2003).
[9] P. Ghenuche, R. Quidant, G. Badenes, Opt. Lett. **30**, 1882 (2005).
[10] G. S. Chen, C. B. Boothroyd, C. J. Humphreys, Appl. Phys. Lett., **62**, 1949 (1993).
[11] Y.E. Guan, A.J. Pedraza, Nanotech., **16**, 1612 (2005).
[12] J. Koch, F. Korte, C. Fallnich, A. Ostendorf, B. N. Chichkov, Opt. Eng. **44**, 051103 (2005).
[13] A. Pereira, A. Cros, P. Delaporte, S. Georgiou, A. Manousaki, W. Marine, M. Sentis, Appl. Phys. A **79**, 1433 (2004),.
[14] R. Le Harzic, Opt. Express, **13**, 6651 (2005).
[15] J. Jersch, K. Dickmann, Appl. Phys. Lett. **68**, 868 (1996).
[16] Eric Diebold, Nathan Mack, Stephen Doorn, Eric Mazur, Langmuir, 1790-1794, 2009
[17] S. J. Henley, J. D. Carey, S. R. P Silva, Appl. Phys. **88**, 081904 (2006).
[18] S. J. Henley, J. D. Carey, S. R. P Silva, Applied Surface Science **253**, 8080 (2007).
[19] A. Taflove, S. C. Hagness, Computational Electrodynamics: The Finite-Difference Time-Domain Method, Artech House, Boston, (2000).
[20] P. B. Johnson, and R. W. Christy, Phys. Rev. B, **6**, 4370 (1972).
[21] A.Vial, A.S. Grimault, D. Macias, D.Barchiesi, M. I. Chapelle, Phys. Rev. B **71**, 085416 (2005).
[22] E. D. Palik, Handbook of optical constants of solids, Acad. Press, San Diego (1998).
[23] M. K. Hossain, K. Shibamoto, K. Ishioka, M. Kitajima, T. Mitani, S. Nakashima, Journal of Luminescence **122**, 792 (2007).
[24] Jin Z. Zhang & Cecilia Noguez, Plasmonics **3**, 127 (2008).
[25] N. Nedyalkov, T. Sakai, T. Miyanishi, M. Obara, J. Phys. D **39**, 5037 (2006).

*Corresponding author: semra007@ yahoo.com